

# PolarAir: A Compressed Sensing Scheme for Over-the-Air Federated Learning

Michail Gkagkos, Krishna R. Narayanan, Jean-Francois Chamberland, Costas N. Georghiades  
Department of Electrical and Computer Engineering, Texas A&M University

**Abstract**—We explore a scheme that enables the training of a deep neural network in a Federated Learning configuration over an additive white Gaussian noise channel. The goal is to create a low complexity, linear compression strategy, called PolarAir, that reduces the size of the gradient at the user side to lower the number of channel uses needed to transmit it. The suggested approach belongs to the family of compressed sensing techniques, yet it constructs the sensing matrix and the recovery procedure using multiple access techniques. Simulations show that it can reduce the number of channel uses by  $\sim 30\%$  when compared to conveying the gradient without compression. The main advantage of the proposed scheme over other schemes in the literature is its low time complexity. We also investigate the behavior of gradient updates and the performance of PolarAir throughout the training process to obtain insight on how best to construct this compression scheme based on compressed sensing.

## I. INTRODUCTION

### A. Federated Learning and Over-the-Air Federated Learning

Federated Learning (FL) was first introduced as Federated Optimization in [1]. The main idea is that the workers use their available data to solve a Machine Learning (ML) task and the Parameter Server (PS) orchestrates the system by sending the current model to workers. In addition, there are some characteristics that describe FL. For example, the samples on each worker can be drawn from a different distribution and the number of available data at each worker may differ by orders of magnitude, known as non-i.i.d. and unbalanced datasets, respectively. The term Federated Learning was established in [2, 3], and FedAvg [4] is the original FL algorithm. The basic steps of FL are as follows. The PS selects a fraction of the workers in the system to join the training and broadcasts the current model. Then, the workers use their available data to calculate local model updates. The average of the updated models is computed by the PS, after receiving messages from the participating workers. The information sharing step is called the communication round. The ML training task goes back and forth between the workers and the PS; training terminates after a certain accuracy is achieved. The main bottleneck in this framework is the communication cost. To alleviate it, the algorithm in [4] has workers update their models locally for  $E$  epochs before sending their updated models to the PS. Alternatively, in the FedPAQ scheme introduced in [5], local updates and quantization are applied to lower the cost.

A majority of the algorithms in FL assume that users communicate to the PS using a medium access control (MAC) layer protocol that prevents interference between users. Therefore, each user in the network can use digital coding and modulation techniques to reliably communicate the compressed quantized gradients over a noisy channel. However, existing literature related to distributed sensing has shown that the superposition nature of the wireless medium can be exploited to directly compute functions (in particular, the sum over the complex field) of each user’s modulated data [6, 7, 8, 9].

The superposition property of the wireless channel has been exploited by Amiri and Gunduz for computing the sum of gradients in FL under the name of over-the-air computation in [10]. This scheme sparsifies the gradient and then applies compressed sensing (CS) techniques to create messages. A scaled version of the sketch is transmitted over a synchronous multiple access AWGN channel, and a noisy sum of the sketches is received at the PS. We refer to the received signal as the measurement vector. In this scheme, Approximate Message Passing (AMP) is used to recover the sum of the gradients from the measurement vector. They call this algorithm an analog computation scheme since the transmitted values are unquantized real numbers. Amiri and Gunduz show that the analog scheme in [10] can achieve better performance than the digital schemes in SignSGD [11], QSGD [12]. Similar ideas have been applied to Single Input Single Output (SISO) fading channels [13], and to Multiple Input Multiple Output (MIMO) channels [14]. More recent algorithms in this area include those described in [15, 16, 17, 18, 19] and the references therein.

### B. Main Contributions

In the three schemes found in [10, 13, 14], the authors aim to train a Neural Network (NN) to classify images of the MNIST dataset. Since the classification of this dataset can be achieved by a NN with a small number of parameters, AMP can be used to recover the sum of sparse vectors. In the present article, we consider the task of classifying images of the CIFAR-10 dataset [20]. This ML task is more challenging and, to reach this goal, we use one of the Residual Networks [21, 22], which contains around 270,000 parameters. Since the time complexity of AMP scales linearly with the length of the sparse vector, a low-complexity alternative to AMP is desirable. Hence, we propose an algorithm, called PolarAir, that combines  $K$ -sparsification and CS, in a manner akin to [23] and [24], to train the ResNet20 [22] over the AWGN

This material is based upon work supported, in part, by the National Science Foundation (NSF) under Grants CCF-2131106 & CNS-2148354, and by Qualcomm Technologies, Inc., through their University Relations Program.

medium. The time complexity of the proposed scheme, and the scheme in [10], is  $\mathcal{O}(K^3 + K^2 \log N)$  and  $\mathcal{O}(MN)$ , respectively, where  $N$  is the length of the gradient, and  $K \ll N$  is sparsity and  $M$  is the number of measurements. Also, we examine the performance of the CS scheme during the training phase. Our findings provide new insights on how to construct CS algorithms for Over-the-Air FL.

## II. SYSTEM MODEL

We consider a wireless network with  $W$  mobile devices called workers, and one remote PS. Workers communicate only with the PS. We denote the collection of all available data in the network by  $\mathbf{D}$ , and the set of available data to worker  $w$  by  $\mathbf{D}_w \subset \mathbf{D}$ . The goal is to train a ML model using distributed data available at each worker node  $w$ . This is accomplished by having workers communicate gradients to the PS sequentially, through several update rounds. Each communication round consists of three operations. First the PS broadcasts the parameters of the current model  $\theta_t$  to all the workers through a reliable communication scheme. Note that this assumption has appeared in previously published work, e.g., [10]. Each worker then employs a subset of their locally available data  $B_w(t) \subset \mathbf{D}_w$  (also known as a batch) together with the current model to compute a gradient  $\mathbf{g}_w(\theta_t)$ . This gradient is then compressed and encoded into the signal  $\mathbf{x}_w(t)$ , which is transmitted to the PS using the (synchronous) multiple access AWGN channel. The signal received at the PS during round  $t$  is

$$\mathbf{y}(t) = \sum_{w=1}^W \mathbf{x}_w(t) + \mathbf{z}(t) \quad (1)$$

where  $\mathbf{x}_w(t) \in \mathbb{R}^M$  is the channel input transmitted by worker  $w$ , which is a function of the gradient,  $\mathbf{y}(t) \in \mathbb{R}^M$  is the received signal and  $\mathbf{z}(t)$  is the AWGN vector with independent and identically distributed (i.i.d.)  $N(0, 1)$  entries. After the training step, the updated model is multicasted to the workers by the PS through a noiseless medium.

The recovery of the average of the  $W$  gradients, i.e.,  $\frac{1}{W} \sum_{w=1}^W \mathbf{g}_w(\theta_t)$ , can be viewed as a computation problem over a MAC [7]; this problem has been studied in the sensor networks literature [8], [6]. In the present context, our goal is to minimize the length of the vector  $\mathbf{x}_w(t)$  that can be used to transmit the gradient, without losing in terms of the test accuracy. To achieve that, we apply a top- $K$  sparsification in conjunction with a CS-based signaling scheme similar to [23, 24]. We focus on an elementary channel model to highlight the main idea behind PolarAir. Nevertheless, it is possible to create extensions of the proposed scheme suited to more intricate channel models (see, e.g., [13]).

## III. POLARAIR

The proposed scheme borrows ideas from [10], and the main contribution of this paper is the CS scheme described in Section IV. The main ideas are a top- $K$  sparsification step, which increases the amount of zeros in the gradient, and a CS encoding step that captures the sparse gradient by taking linear measurements. The first component of the compression

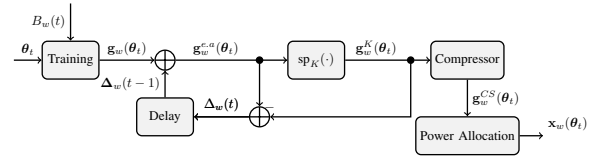


Fig. 1. The protocol all workers follow; similar to the architecture in [10]

algorithm is motivated by the fact that sparse updates act in a manner similar to a regularization term. Then, leveraging CS techniques make sense because a  $K$ -sparse vector of length  $N$  can be stored by taking  $\mathcal{O}(K \log \frac{N}{K})$  linear measurements [25]. Since the map from the sparse vector to its measurement vector is linear, the sum of the sparse gradients can be recovered from the sum of their corresponding measurement vectors, under suitable conditions. More specifically, our goal is to recover the largest  $K$  values of the sum of the  $W$  transmitted  $K$ -sparse vectors. In this paper, “ $K$  largest values” means the  $K$  largest values in magnitude. Also, we note that each worker has a different dataset and, hence, we expect the sum of  $W$  gradient vectors, each with at most  $K$  non-zero entries, to yield an aggregate vector with at most  $KW$  non-zero entries. Still, we only wish to recover the strongest  $K$  values in this group.

### A. Worker

All workers involved in the training process follow the same protocol for every communication round. We restrict our attention to worker  $w$  and communication round  $t$  to describe the steps of PolarAir. A block diagram of the procedure at the worker side is given in Fig. 1. First, the worker receives the model parameters  $\theta_t$  from the PS. Then, based on the batch size,  $|B_w(t)| \leq |\mathbf{D}_w|$ , worker  $w$  trains the current model; that is, it computes the gradient  $\mathbf{g}_w(\theta_t)$ . To keep the estimator unbiased, the local accumulation error is added to the gradient and the resulting vector becomes

$$\mathbf{g}_w^{e.a.}(\theta_t) = \mathbf{g}_w(\theta_t) + \Delta_w(t-1), \quad (2)$$

where  $\Delta_w(t-1)$  is the error defined in (3), with initial condition  $\Delta_w(0) = \mathbf{0}$  at time  $t = 0$ . Furthermore, a top- $K$  sparsification operation is applied, and the resulting vector of length  $N$  has only  $K$  non-zero entries. We denote the top- $K$  sparsification function as  $\text{sp}_K(\cdot)$  and the input and output of this function are indicated by  $\mathbf{g}_w^{e.a.}(\theta_t)$  and  $\mathbf{g}_w^K(\theta_t)$ , respectively. Note that  $K$  is fixed during the training process, and it is known to all participants a priori. The next step is to compute the error between the dense vector  $\mathbf{g}_w^{e.a.}(\theta_t)$  and the sparsified vector  $\mathbf{g}_w^K(\theta_t)$ . The error is indicated by  $\Delta_w(t)$  and can be computed as

$$\Delta_w(t) = \mathbf{g}_w^{e.a.}(\theta_t) - \mathbf{g}_w^K(\theta_t) \quad (3)$$

Next, a CS scheme, similar to [24] and [23], is used to reduce the dimension of vector  $\mathbf{g}_w^K(\theta_t)$  from  $N$  to  $M_t < N$ . For the time being, we treat the CS algorithm as a black box; the details of the adopted scheme are available in Section IV. We denote the output of the CS encoding by  $\mathbf{g}_w^{\text{CS}}(\theta_t) \in \mathbb{R}^{M_t}$ . Because the values of  $\mathbf{g}_w^{\text{CS}}(\theta_t)$  are unconstrained, the resulting

vector does not satisfy a power constraint. Thus, we apply power control in a manner akin to the Mean-Removal power control of [10]. A main difference between our CS scheme and the scheme in [10] is that the former is adaptive. In other words, the number of measurements increases as the performance of the recovery algorithm decreases. We explain when and how to increase  $m_t$  in Section V. The average power of the symbol is set to  $P$  and, therefore, the power of the channel input  $\mathbf{x}_w(t)$  is linear in the number of measurements. Particularly, the power of the transmitted signal is  $\|\mathbf{x}_w(t)\|_2^2 = P(m_t + 2) = PM_t$ . By establishing the power constraint of the problem, we can proceed with the power control algorithm. The first step of algorithm in [10] is to compute the mean of the measurement vector, i.e.,  $\mu_w(t) = \frac{1}{m} \sum_{i=1}^m g_{i,w}^{\text{CS}}(\boldsymbol{\theta}_t)$ , and subtract it from the output of the CS algorithm,  $\mathbf{g}_w^{m.r.}(\boldsymbol{\theta}_t) = \mathbf{g}_w^{\text{CS}}(\boldsymbol{\theta}_t) - \mu_w(t)\mathbf{1}_m$ . Then the channel input takes the form,

$$\mathbf{x}_w(t) = \left[ \sqrt{a_w(t)} \quad \sqrt{a_w(t)}\mu_w(t) \quad \sqrt{a_w(t)}\mathbf{g}_w^{m.r.}(\boldsymbol{\theta}_t) \right]^\top, \quad (4)$$

where  $a_w(t)$  is a scale factor chosen to satisfy the average symbol power constraint.

$$\frac{\|\mathbf{x}_w(t)\|_2^2}{m_t + 2} = a_w(t) \left( 1 + \mu_w^2(t) + \|\mathbf{g}_w^{m.r.}(\boldsymbol{\theta}_t)\|_2^2 \right) = P. \quad (5)$$

As a result,  $a_w(t)$  is specified by

$$a_w(t) = \frac{P(m_t + 2)}{1 + (m_t - 1)\mu_w^2(t) + \|\mathbf{g}_w^{\text{CS}}(\boldsymbol{\theta}_t)\|_2^2}. \quad (6)$$

Finally, workers form  $\mathbf{x}_w(t)$  and transmit it over the MAC.

### B. Parameter Server

Because all workers send their data synchronously, the PS receives the sum of the  $W$  transmitted signals. The goal is to recover a  $K$ -sparse vector from observation vector  $\mathbf{y}(t)$ . We denote the part of the received signal that corresponds to the sum of the measurement vectors by  $\mathbf{y}_3^{M_t}(t) = [y_3(t) \quad y_4(t) \quad \cdots \quad y_{M_t}(t)]$ . The first step that the PS takes is to add the second value of the channel output, i.e.,  $y_2(t) = \sum_{w=1}^W \sqrt{a_w(t)}\mu_w + z_2(t)$ , to  $\mathbf{y}_3^{M_t}(t)$  and divide the result by  $y_1(t) = \sqrt{a_w(t)} + z_1(t)$ . The resulting vector is given by

$$\tilde{\mathbf{y}}(t) = \frac{1}{y_1(t)} (\mathbf{y}_3^{M_t}(t) + y_2(t)\mathbf{1}_{M_t-3}). \quad (7)$$

Then,  $\tilde{\mathbf{y}}(t)$  is passed to the recovery algorithm. The objective is to output a  $K$ -sparse vector, which hopefully contains the largest entries of the sum of the gradients. Recall that the sum of the  $K$ -sparse vectors is likely to be a vector with  $K' \in [K : KW]$  non-zero entries. As a result,  $K' - K$  entries of  $\mathbf{g}^k(\boldsymbol{\theta}_t)$  act as noise. Let us define  $\text{supp}(\mathbf{g}^k(\boldsymbol{\theta}_t))$  and  $\mathcal{A}$  to be the support of  $\mathbf{g}^k(\boldsymbol{\theta}_t)$  and the indices that correspond to the largest values of  $\mathbf{g}^k(\boldsymbol{\theta}_t)$ , i.e.,

$$\text{supp}(\mathbf{g}^k(\boldsymbol{\theta}_t)) = \{j : g_j^k(\boldsymbol{\theta}_t) \neq 0\} \text{ and } \mathcal{A} = \text{sp}_K(\mathbf{g}^k(\boldsymbol{\theta}_t)).$$

Then, the goal of the algorithm is to recover the indices in

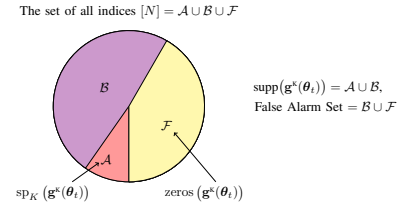


Fig. 2. Illustration of Active Indices in the False Alarm Set, where  $\mathcal{F}$  is the set of the non-active indices of  $\mathbf{g}^k(\boldsymbol{\theta}_t)$ .

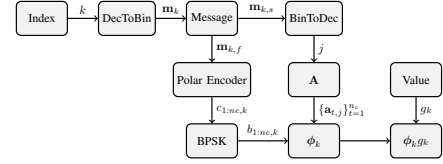


Fig. 3. Encoding procedure of the  $k$ th active index

$\mathcal{A}$  and the corresponding values. Nevertheless, if the decoder outputs an index that belongs to  $\mathcal{B} = \text{supp}(\mathbf{g}^k(\boldsymbol{\theta}_t)) \setminus \mathcal{A}$  then, from training point of view, this index will contribute to the convergence of the CNN. We define  $\mathcal{B}$  as the *Active Indices in the False Alarm Set*. For example, let  $\mathbf{g}^k(\boldsymbol{\theta}_t) = [-3, 1, 0, -0.01, 4, 0, 0, 0.5]$  and  $K = 2$ , then  $\mathcal{A} = \{1, 5\}$  and  $\mathcal{B} = \{2, 4, 8\}$ . Figure 2 shows the relation between the sets. After this step, an estimate of the gradient  $\mathbf{g}^k(\boldsymbol{\theta}_t)$  is available and the PS updates the parameters as  $\boldsymbol{\theta}_{t+1} = \boldsymbol{\theta}_t - \alpha_t \hat{\mathbf{g}}^k(\boldsymbol{\theta}_t)$ , where  $\alpha_t$  is the learning rate and  $\hat{\mathbf{g}}^k(\boldsymbol{\theta}_t)$  denotes the estimate. Finally, the updated model is broadcast to the workers, and the  $t + 1$  communication round begins.

## IV. COMPRESSED SENSING SCHEME

In this section, we propose the CS algorithm that is used to compress the sparse gradient. Throughout this section, the dependence of  $t$  is omitted for notational convenience. Since our scheme borrows ideas from [24], we only outline the main functionality here. We want to focus on the behaviour of the algorithm in the FL problem, and not on the structure of the CS algorithm itself.

### A. Compression at the Workers Side

The model in the CS literature has the form  $\mathbf{y} = \Phi \mathbf{x} + \mathbf{n}$ , where  $\mathbf{x} \in \mathbb{R}^N$  is a  $K$ -sparse vector,  $\Phi \in \mathbb{R}^{M \times N}$  is a short-wide matrix,  $\mathbf{n}$  is the measurement noise, and  $\mathbf{y}$  is the measurement vector. The designer of a CS algorithm aims to construct a measurement matrix and a recovery algorithm to solve a particular CS problem. In our scheme, one can generate the columns of the measurement matrix  $\Phi$  on the fly. Note that the active indices are available after the sparsification step. Hence, each worker only needs to generate the active columns of  $\Phi$ , thereby avoiding the vector-matrix multiplication. Along these lines, we describe how one can generate the  $k$ th column of  $\Phi$  using the binary representation of  $k$ . The encoding process of the  $k$ th index is illustrated in Fig. 3.

Every vector  $\mathbf{g}_w^k(\boldsymbol{\theta})$  has  $K$  non-zero entries and, hence, it can be constructed as the weighted sum of  $K$  standard basis vectors. For each such vector summand, the integer location

$k$  of the non-zero entry admits a binary representation  $\mathbf{m}_k$ . The length of the the binary sequence  $\mathbf{m}_k$  is  $B = \lceil \log_2 N \rceil$  bits, possibly with leading zeros. Every such binary sequence is split into two parts:  $\mathbf{m}_{k,f}$  and  $\mathbf{m}_{k,s}$  of lengths  $B_f$  and  $B_s$ , respectively. Based on the decimal representation of  $\mathbf{m}_{k,s}$ , index  $k$  chooses one of the  $J$  columns within the spreading dictionary  $\mathbf{A}_i \in \{\pm\sqrt{1/N}\}^{L \times J}$ ,  $i \in [n_c]$ , where  $n_c$  represents the length of the code and  $L$  is the length of the spreading sequences. The entries of  $\mathbf{A}_i$  are drawn independently from the set  $\{\pm\sqrt{1/N}\}$  with equal probability. The actual spreading operation for the  $i$ th coded bit is described next. The decimal representation of  $\mathbf{m}_{k,s}$  is also employed to pick the values of the frozen bits for polar encoding.

To facilitate list decoding,  $\mathbf{m}_{k,f}$  is padded with  $r$  cyclic redundancy check (CRC) bits resulting in a message length of  $r + B_f$  bits. A polar encoder maps this CRC augmented sequence into a codeword  $\mathbf{c}_k$  of length  $n_c$ . Each coded bit of  $c_{i,k}$ ,  $i \in [n_c]$  is then BPSK modulated,  $b_{i,k} \in \{-1, +1\}$ . Finally,  $b_{i,k}$  is spread by the spreading sequence  $\mathbf{a}_{i,k}$ , which is determined by  $\mathbf{m}_{k,s}$ . Given this encoding structure, we can see that the measurement matrix  $\Phi$  is composed of columns of the form,

$$[b_1 \mathbf{a}_{1,j}^T \quad b_2 \mathbf{a}_{2,j}^T \quad \cdots \quad b_{n_c} \mathbf{a}_{n_c,j}^T]^T$$

where  $j \in [J]$ . Next, the worker can apply the same methodology to generate the next active column. After  $K$  iterations, the worker has generated the active columns, and it can therefore obtain the compressed version of  $\mathbf{g}_w^k(\theta)$  as

$$\mathbf{g}_w^{\text{CS}}(\theta) = \sum_{k \in \mathcal{K}_w} \phi_k \mathbf{g}_{k,w}^k(\theta) = \Phi \mathbf{g}_w^k(\theta), \quad (8)$$

where  $\mathcal{K}_w$  is the support of  $\mathbf{g}_w^k(\theta)$ . Since all the workers apply the same encoding strategy, the sum of  $W$  such vectors is given by

$$\begin{aligned} \mathbf{g}^{\text{CS}}(\theta) &= \sum_{w=1}^W \Phi \mathbf{g}_w^k(\theta) = \Phi \left( \sum_{w=1}^W \mathbf{g}_w^k(\theta) \right) = \Phi \mathbf{g}^k(\theta) \\ &= \underbrace{\Phi \mathbf{g}_A(\theta)}_{\text{top-}K \text{ entries}} + \underbrace{\Phi \mathbf{g}_B(\theta)}_{\text{other non-zero}} \end{aligned}$$

where  $\mathbf{g}_A(\theta)$  is the vector that the PS aims to recover.

### B. Recovery Algorithm at the PS

The PS receives  $\mathbf{y}$  found in (1) and, after the pre-processing step discussed in Section III-B, the input to the recovery algorithm is given by (7). The iterative recovery algorithm features a few distinct components; a matched filter, an energy detector, two polar decoders, a least squares estimator, and a successive interference canceller (SIC). We should stress, again, that the sum of  $K$ -sparse signals need not be  $K$ -sparse. However, the objective of the algorithm is to recover the largest  $K$  entries of  $\mathbf{g}^k(\theta)$  or, equivalently,  $\mathcal{A}$ . A block diagram of the recovery algorithm is shown in Fig. 4.

1) *Matched Filter and Energy Detector:* The signal  $\tilde{\mathbf{y}}$  is reshaped in a form amenable to sequence detection as follows,

$$\tilde{\mathbf{Y}} = [\tilde{y}_1 \quad \tilde{y}_2 \quad \cdots \quad \tilde{y}_{n_c}] \quad (9)$$

where  $\tilde{y}_i \in \mathbb{R}^L$ . Section  $\tilde{y}_i$  denotes the received signal corresponding to the  $i$ th polar coded symbol. The sequence detector computes  $Z_{i,j} = \langle \mathbf{a}_{i,j}, \tilde{y}_i \rangle$  for every pair  $(i, j) \in [n_c] \times [J]$ , where  $\mathbf{a}_{i,j}$  is the  $j$ th spreading sequence from the set  $\mathbf{A}_i$ . We call  $Z_{i,j}$  the estimate of the  $i$ th coded bit, given that  $\mathbf{a}_{i,j}$  is active. The sequence detector iterates over all  $(i, j)$  pairs and picks  $K - S$  sequence with the largest  $E_j = \sum_{i=1}^{n_c} |Z_{i,j}|^2$ , where  $S$  is the number of indices that the iterative algorithm has subtracted in the previous SIC iterations.

2) *Detection of Polar Codewords:* When spreading sequence  $\mathbf{a}_{i,j}$  is active, the elements of  $Z_{1:n_c,j}$  can act as estimates for the polar coded bits  $b_{1:n_c,j}$ . Yet, the sign of  $x_k$  is unknown and, hence, there is a need to run two list decoders. The inputs to these list decoders are  $Z_{1:n_c,j}$  and  $-Z_{1:n_c,j}$ , respectively. The list decoder verifies the CRC constraint for every decoded codeword. If two or more messages satisfy the checks, the most likely message is passed to the next step.

3) *Estimation of Non-Zero Entries in  $\mathbf{g}^{\text{CS}}(\theta)$ :* Since no prior distribution is available for the values of the gradient and  $K \ll N$ , we can apply least-squares (LS) estimation.

4) *Successive Interference Cancellation:* The contributions of the recovered non-zero entries in the sparse signal are removed from the received signal in the spirit of SIC. The residual is then passed to the energy detector for the next decoding round. This process continues until  $K$  indices are recovered successfully, or there is no improvement between consecutive rounds, or the maximum number of iterations is reached.

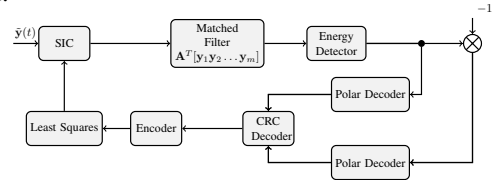


Fig. 4. The block diagram of the Recovery Algorithm.

## V. EXPERIMENTS

To evaluate the performance of the algorithm, we use it to solve a classification problem. Specifically, the PS and workers wish to train a CNN to classify the images of the CIFAR-10 dataset [20]. This dataset contains 60,000 RGB images of size  $32 \times 32$  pixels, divided into 10 classes. Since the goal of this article is to design a FL scheme for a large model, we use the ResNet20 [22] to classify these images. This network consists of  $N = 269,722$  parameters; we select  $K = 270$ . The FL setting includes a PS,  $W = 8$  workers and, every worker possesses  $|\mathbf{D}_w| = 6144$  examples. The data samples are chosen randomly and are distinct at each worker (i.i.d. datasets)<sup>1</sup>. We use  $|\mathbf{D}_{\text{train}}| = W|\mathbf{D}_w| = 49,152$  examples for the training, and  $|\mathbf{D}_{\text{test}}| = 10,000$  for testing. The batch size is  $B_w(t) = 256$ , and the number of communication rounds per epoch is  $C = 24$ . The parameters are updated by the ADAM optimizer [26] with learning rate  $\text{lr} = 0.01$ . We compare our

<sup>1</sup>Since the compression algorithm does not exploit the correlation between the gradients at the worker side, it can be applied to FL problems with non-i.i.d. datasets. We anticipate a decrease in performance in such cases.

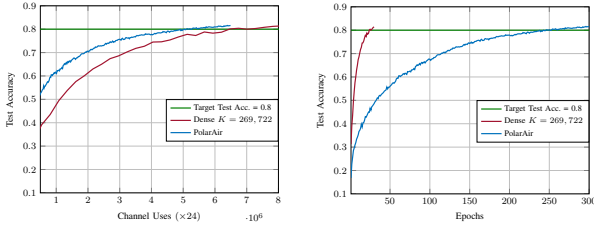


Fig. 5. Test Accuracy as a function of Channel Uses. Fig. 6. Test Accuracy as a function of Epochs.

algorithm with a scenario, where a genie gives the average of the  $W$  sparse vectors to the PS, i.e.,  $\frac{1}{W}\mathbf{g}^K(\boldsymbol{\theta}_t)$  is directly available at the PS (no compression). The PS uses  $\frac{1}{W}\mathbf{g}^K(\boldsymbol{\theta}_t)$  to update the model. We denote this scheme by *Dense*. We set the target test accuracy to be 0.8, and we count the number of channel uses needed from each scheme to achieve the target accuracy.

For PolarAir, we choose the initial parameters to be  $B_f = 10$ ,  $B_s = 9$ ,  $J = 2^{B_f} = 1024$ ,  $L = 400$ ,  $n_c = 32$ ,  $n_L = 2$  and  $P = 1000$ . Therefore, the initial number of measurements is  $m_1 = 12,800$ , which is 20 times less than  $N$ . Let  $\hat{\mathcal{A}}_{c,e}$  be the set of recovered indices after communication round  $c \in [C]$  and during epoch  $e$ . We increase the number of measurements if, at the end of the epoch,  $Q \triangleq \frac{1}{C} \sum_{c=1}^C |\hat{\mathcal{A}}_{c,e}| \leq \frac{K}{2}$ . A naive policy to increase the number of measurements,  $M = Ln_c$ , is given by

$$(L, n_c) = \begin{cases} (L, n_c + 32), & \text{if } Q \leq \frac{K}{2} \text{ for the first time} \\ (L + 100, n_c), & \text{otherwise.} \end{cases}$$

That means, that the first time  $Q \leq \frac{K}{2}$ , PolarAir increases the length of the codeword  $n_c$ . Then,  $n_c$  remains fixed, and only the length of the spreading sequence grows. A more optimal way to design  $Q$  and the update policy is left for future work.

Figure 5 depicts the test accuracy as a function of the channel uses. The figure clearly shows that the CS based scheme outperforms *Dense*. On the other hand, Fig. 6 presents the test performance of the two schemes as a function of the number of epochs. As we expected, *Dense* converges faster than PolarAir. From a wireless communication point of view, we are interested in the number of channel uses rather than the number of epochs; this better captures the radio resources (spectrum and energy) utilized by the workers. It should be noted that we do not compare our scheme with the one in [10] because it is impractical to store a Gaussian measurement matrix with dimensions  $M \times N$ , where  $N = 269,722$  and  $M \geq 12800$ ; their algorithm cannot be implemented for the present setting. We give several graphics in the rest of this section that illustrate the behavior of the proposed scheme and the sum of the sparse vectors during training. These findings will aid in the development of task-specific compression algorithms.

First we investigate the number of non-zero values in the sum of the gradients  $\mathbf{g}^K(\boldsymbol{\theta}_t)$ . Figure 7 plots the average of the total number of active indices, i.e.  $\mathcal{A} \cup \mathcal{B}$ , (see Fig 2) as a function of epochs. Note that  $K = 270$  and  $W = 8$ , hence

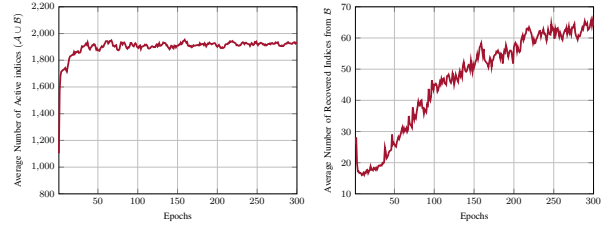


Fig. 7. Average number of active indices as a function of epochs. Fig. 8. Average Number of Recovered Indices from  $\mathcal{B}$

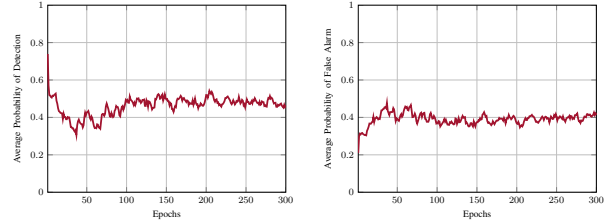


Fig. 9. Average probability of Detection. Fig. 10. Average probability of False Alarm.

there can be at most  $KW = 2160$  non-zero values in  $\mathbf{g}^K(\boldsymbol{\theta}_t)$ . It is clear that after the 50th epoch the average number of nonzero values is around 1900. Since the objective of the CS component is to retrieve  $K = 270$ , the remaining  $1900 - K = 1630$  values essentially behave like noise. This indicates that, as the number of epochs increases, so does the noise in the CS problem, creating the need for further measurements.

Next, we are interested in the performance of the CS scheme. The Detection  $P_d$  and False Alarm  $P_{fa}$  probability of error of the recovery algorithm are shown in Fig. 9 and Fig. 10. Interestingly, as the number of epochs increases, the  $P_d$  and  $P_{fa}$  converge to 0.5 and 0.4, respectively. Values that show poor performance from CS perspective. However, the test accuracy of the model increases, (see Figures 5 & 6). The reason behind this contradiction is given in Fig. 8, where the average number of recovered indices that belongs to *Active Indices in the False Alarm Set*, i.e.  $\hat{\mathcal{B}}$ , as a function of epochs is illustrated. We denote  $\hat{\mathcal{B}}$  all the indices that the recovery algorithm recovers and belongs to  $\mathcal{B}$ . Clearly, when this number increases, the performance of the recovery algorithm suffers. However, because at least some of the workers communicate these indices, recovering them and using them for a gradient update is advantageous from a training standpoint. Further analysis and additional comments are omitted due to space limitations.

## VI. SUMMARY

This article demonstrates that multiple access techniques can be leveraged to construct CS algorithms that can compress gradient updates for models that have thousands of parameters. This approach enables over-the-air FL at scale. Secondly, we offer a methodology based on how the gradient vectors change over epochs to give insight into parameter selection for CS-based, over-the-air FL problems.

## REFERENCES

- [1] J. Konečný, B. McMahan, and D. Ramage, “Federated optimization: distributed optimization beyond the data-center,” *arXiv preprint arXiv:1511.03575*, 2015.
- [2] J. Konečný, H. B. McMahan, F. X. Yu, P. Richtarik, A. T. Suresh, and D. Bacon, “Federated learning: Strategies for improving communication efficiency,” in *NIPS Workshop on Private Multi-Party Machine Learning*, 2016.
- [3] H. Brendan McMahan, Eider Moore, Daniel Ramage, and Blaise Agüera y Arcas, “Federated learning of deep networks using model averaging,” *CoRR*, vol. abs/1602.05629, 2016.
- [4] H. B. McMahan, Eider Moore, D. Ramage, S. Hampson, and B. A. Y. Arcas, “Communication-efficient learning of deep networks from decentralized data,” in *AISTATS*, 2017.
- [5] A. Reisizadeh, A. Mokhtari, H. Hassani, A. Jadbabaie, and R. Pedarsani, “FedPAQ: A communication-efficient federated learning method with periodic averaging and quantization,” in *International Conference on Artificial Intelligence and Statistics, AISTATS 2020*. 2020, vol. 108, pp. 2021–2031, PMLR.
- [6] Omid Abari, Hariharan Rahul, and Dina Katabi, “Over-the-air Function Computation in Sensor Networks,” *arXiv e-prints*, p. arXiv:1612.02307, Dec. 2016.
- [7] B. Nazer and M. Gastpar, “Computation over multiple-access channels,” *IEEE Transactions on Information Theory*, vol. 53, no. 10, pp. 3498–3516, 2007.
- [8] M. Goldenbaum and S. Stanczak, “Robust analog function computation via wireless multiple-access channels,” *IEEE Transactions on Communications*, vol. 61, no. 9, pp. 3863–3877, 2013.
- [9] M. P. Wilson, K. Narayanan, and G. Caire, “Joint source channel coding with side information using hybrid digital analog codes,” *IEEE transactions on information theory*, vol. 56, no. 10, pp. 4922–4940, 2010.
- [10] M. M. Amiri and D. Gündüz, “Machine learning at the wireless edge: Distributed stochastic gradient descent over-the-air,” in *2019 IEEE International Symposium on Information Theory (ISIT)*, 2019, pp. 1432–1436.
- [11] J. Bernstein, Y.-X. Wang, K. Azizzadenesheli, and A. Anandkumar, “SIGNSGD: Compressed optimisation for non-convex problems,” in *ICML*, 2018, pp. 559–568.
- [12] D. Alistarh, D. Grubic, J. Li, R. Tomioka, and M. Vojnovic, “QSGD: Communication-efficient SGD via gradient quantization and encoding,” in *Advances in Neural Information Processing Systems*, 2017, vol. 30.
- [13] M. M. Amiri and D. Gündüz, “Federated learning over wireless fading channels,” *IEEE Transactions on Wireless Communications*, vol. 19, no. 5, pp. 3546–3557, 2020.
- [14] Y.-S. Jeon, M. M. Amiri, J. Li, and H. V. Poor, “A compressive sensing approach for federated learning over massive mimo communication systems,” *IEEE Transactions on Wireless Communications*, vol. PP, pp. 1–1, 11 2020.
- [15] A. Abdi, Y. M. Saidu, and F. Fekri, “Analog compression and communication for federated learning over wireless MAC,” in *2020 IEEE 21st International Workshop on Signal Processing Advances in Wireless Communications (SPAWC)*, 2020, pp. 1–5.
- [16] R. Paul, Y. Friedman, and K. Cohen, “Accelerated gradient descent learning over multiple access fading channels,” *IEEE Journal on Selected Areas in Communications*, vol. 40, no. 2, pp. 532–547, 2022.
- [17] D. Fan, X. Yuan, and Y.-J. A. Zhang, “Temporal-structure-assisted gradient aggregation for over-the-air federated edge learning,” *IEEE Journal on Selected Areas in Communications*, vol. 39, no. 12, pp. 3757–3771, 2021.
- [18] Y.-S. Jeon, M. M. Amiri, and N. Lee, “Communication-efficient federated learning over MIMO multiple access channels,” *IEEE Transactions on Communications*, vol. 70, no. 10, pp. 6547–6562, 2022.
- [19] C.-Z. Lee, L. P. Barnes, and A. Ozgur, “Over-the-air statistical estimation,” *IEEE Journal on Selected Areas in Communications*, vol. 40, no. 2, pp. 548–561, 2022.
- [20] A. Krizhevsky, “Learning multiple layers of features from tiny images,” *University of Toronto*, 05 2012.
- [21] K. He, X. Zhang, S. Ren, and J. Sun, “Deep residual learning for image recognition,” in *Proceedings of the IEEE conference on Computer Vision and Pattern Recognition*, 2016, pp. 770–778.
- [22] Y. Idelbayev, “Proper ResNet implementation for CIFAR10/CIFAR100 in PyTorch,” .
- [23] A. K. Pradhan, V. K. Amalladinne, K. R. Narayanan, and J.-F. Chamberland, “Polar coding and random spreading for unsourced multiple access,” in *ICC 2020 - 2020 IEEE International Conference on Communications (ICC)*, 2020, pp. 1–6.
- [24] M. Gkagkos, A. K. Pradhan, V. Amalladinne, K. Narayanan, J.-F. Chamberland, and C. N. Georghiadis, “Approximate support recovery using codes for unsourced multiple access,” in *2021 IEEE International Symposium on Information Theory (ISIT)*, 2021, pp. 2948–2953.
- [25] Y. C. Eldar and G. Kutyniok, *Compressed Sensing: Theory and Applications*, Cambridge University Press, 2012.
- [26] D. P. Kingma and J. Ba, “Adam: A method for stochastic optimization,” in *ICLR (Poster)*, 2015.